J. Min. Metall. Sect. B-Metall. 54 (3) B (2018) 283 - 290

Journal of Mining and Metallurgy, Section B: Metallurgy

INVESTIGATION OF DISSOLUTION RESISTANCE OF BLANK AND GAS-NITRIDED CARBON STEELS IN STATIONARY SAC305 SOLDER ALLOY MELT

M. Benke*, Zs. Salyi, G. Kaptay

* University of Miskolc, Institute of Physical Metallurgy, Metalforming and Nanotechnology, Miskolc-Egyetemvaros, Hungary

(Received 18 September 2017; accepted 22 October 2018)

Abstract

The objective of the present study is to investigate the suitability of a series of gas-nitrided steels with varying C content as candidates for wettable selective soldering tool materials with enhanced lifetime. ε and γ' iron-nitrides were formed by gas nitriding on quenched and tempered DC04, C45, CK60 and S103 type steels. Contact angle measurements revealed that all four nitrided steels exhibit good wetting with SAC305 solder melt. In order to investigate the dissolution reactions between the nitrided steels and the solder alloy, an equipment was assembled in which the samples were submerged into stationary SAC305 solder melt for different time durations. Evidences of dissolution reactions and other degradation processes were searched for using scanning electron microscopy and energy dispersive X-ray spectroscopy. It was observed that no Fe dissolution occurred between the samples and stationary SAC305 solder melt during continuous tests with durations up to 20 days. Furthermore, no other visible degradation reactions occurred between the samples and melt during the experiments. It was concluded that gas-nitrided steels show good wetting with Sn-based solder melts which is combined with excellent resistance against Fe dissolution in a high Sn-containing molten solder. Thus, gas-nitrided steels/iron can be potential materials for wettable selective soldering tools with improved lifetime.

Keywords: *Iron-nitride; Selective soldering, Wetting; SAC305, Dissolution*

1. Introduction

Selective soldering technique can be divided into two groups based on the mode the solder melt is carried to the target area. During selective hand soldering, the solder is molten by the soldering iron tip to which a drop of solder attaches, and then it is lifted and transferred to the target area by the operator. In this case, proper wetting between the molten solder and the soldering iron tip ensures that the solder droplet is lifted. In the case of selective wave soldering, the molten solder flows through the nozzle, on which a wave of melt is formed. If the nozzle is of wettable type, the melt drains down all around the nozzle. If the nozzle is of non-wettable type, the melt flows through a spout back into the solder bath. In both groups of selective soldering techniques, the solder alloy melt is in direct contact with the tools.

The core of soldering iron tips is made of Cu which is usually covered with Ni and Fe. In addition, an Sn layer is produced at the end of the tip to improve wetting between the tip and molten solders. Thus, an Fe/Sn interface is formed at the end of the tip. At the Fe/Sn interface, an intermetallic $FeSn_2$ layer is formed which thickens as operation time passes. The thickening of the $FeSn_2$ layer requires atoms of both Sn and Fe. While Sn is provided from the solder melt, Fe atoms are taken from the Fe layer. The continuous dissolution of Fe atoms causes the thinning of the Fe layer and results in pits and ditches on the soldering iron tip surface. Once the Fe layer is perforated, the further degradation involves the dissolution of other elements of the soldering iron as well [1-3].

Wettable selective soldering nozzles are made of iron with low alloying and impurity element concentrations or high purity Armco iron to ensure proper wetting between the soldering tools and solders. Here, the iron gets into direct contact with the solder melt. The reactive Sn-containing solder melts induce the dissolution of Fe atoms from the nozzle into the melt. The dissolution process is enhanced by the erosive effect of the melt flow [4]. This combined degradation mechanism appears macroscopically as the erosion of the soldering nozzle which produces a rugged surface. As the roughness of the nozzle increases, the stability of the solder wave decreases, which leads to a bouncing solder wave. When this occurrs, solder joints cannot be formed any longer

**Corresponding author:fembenke@uni-miskolc.hu*

DOI:10.2298/JMMB170918019B

with precision and the nozzle must be replaced. The major contribution to the economic impact of the soldering tool degradation is not the cost of the tool itself, but the economic loss related to the interruption of a continuous production line required for nozzle replacement.

The degradation of both hand soldering irons and selective wave soldering nozzles was accelerated as the earlier Sn-Pb solder alloys were replaced with the recently developed environmentally friendly Pb-free solders, such as SAC and INNOLOT. It is commonly accepted that the enhanced degradation is attributed to the higher Sn content of the Pb-free alloys, compared to Sn-Pb alloys and the elevated soldering temperature [2-11].

The dissolution of metals submerged in Sn-based solder melts can be reduced through the modification of the solder melt's composition. Nishikawa et al. showed that the addition of Co to Sn-Ag solder alloy effectively reduces the dissolution reaction of Fe plated Cu in Sn-Ag solder melt [11]. However, for most cases, the composition of the solder alloy is designed based on other aspects such as processability, solder joint quality and solder joint reliability [9,12-19]. Thus, the improvement of the selective soldering tools' lifetime cannot be realized on the basis of solder composition modification. Because of that, the most effective way to improve the lifetime of selective soldering tools is to redesign their materials in such a way to suppress the Fe dissolution. J. Watanabe et al. examined the erosion resistance of Fe-MWCNT (Multi Wall Carbon Nanotube) composite in molten Pb-free solder alloy. They found that by applying the Fe-MWNT composite material the resistance against erosion was increased, but wetting was decreased [20]. Although this concept seemed to be promising, the applied composite material is rather costly and its production is complicated, therefore it might not offer a reasonable solution. Finally, the lifetime improvement of selective soldering tools can be realized through redesigning their material by applying cost effective materials and methods. The objective of the present study is to investigate the suitability of gas-nitrided carbon steels as candidates for wettable selective soldering tool materials with enhanced lifetime. The samples were tested for the two basic requirements. First, wetting conditions were characterized between gas-nitrided DC04, C45, CK60 and S103 steels and the SAC305 solder alloy. Afterwards, the resistance of the gas-nitrided steels against dissolution was investigated in stationary SAC305 solder melt.

2. Materials and methods

Four commonly used and commercially available carbon steels were selected for the examinations. The C-content varied in the selected steel series. The nominal compositions of the examined steels are summarized in Table 1.

Table 1. *Nominal compositions of the examined steels [wt%]*

Steel type	C	Mn	Si	P	S
DC04	0.08	0.4	-	0.03	0.03
C45	0.45	0.7	0.3	-	0.03
CK60	0.61	0.8	0.3	-	0.03
S103	1.00-1.10	0.10-0.25	0.10-0.25	max 0.02	max 0.02

For contact angle measurements, plates with dimensions of 8 mm x 9 mm x 3 mm were cut, and for dissolution tests bricks with dimensions of 18 mm x 13 mm x 7 mm were machined from bulk steels. Prior to nitriding, the specimen plates and bricks of C45, CK60 and S103 type steel were quenched and tempered (QT). DC04 type specimens were not heat treated. The austenization and tempering treatments were carried out in an air furnace. The further parameters of the heat treatments are listed in Table 2. The parameters of heat treatments were determined based on the Boehler's catalog [21].

Table 2. *Quenching and tempering parameters of the examined steel types*

Steel type	T_Q [K] (^oC)	T_{Temp} [K] (^oC)	Quenching media
DC04	-	-	-
C45	1133 (860)	873 (600)	Stirred oil
CK60	1108 (835)	873 (600)	Calm oil
S103	1073 (800)	873 (600)	Water

After heat treatments, 0.5 mm thick layers were removed by machining from all sides of the specimens to ensure that the decarburized regions were removed. Iron-nitride was produced on the surface of the samples through gas nitrocarburizing (nitriding from now on) at 823 K (550°C) for 6 hours in an SLR-5 type furnace.

The iron-nitrides produced during gas nitriding were identified through X-ray diffraction (XRD) phase analysis which was performed with a Bruker D8 Advance diffractometer using CoKα radiation, 40 kV tube voltage, and 40 mA tube current.

Contact angles were measured between the iron-nitride layers produced on the steel substrates and SAC305 solder alloy. Before contact angle measurements, the surfaces of the samples were cleaned with a commercial flux (Lux-Tools DIN EN 29454). The samples were placed in an air furnace with a small piece of SAC305 solder alloy on the top. The composition of the SAC305 alloy is given in Table 3.

Table 3. *Composition of the SAC305 solder alloy used for wetting angle measurements and dissolution examinations [wt%]*

Sn	Ag	Cu
96.34	2.95	0.59

After holding the samples at 593 K (320°C) for 20 minutes, they were removed and let cool down. The equilibrium contact angles were measured at room temperature, on both sides of the droplet. If the deviation of the contact angles measured on the two sides of the sample was higher than 10°, the results were neglected. Such deviations originate from surface roughness caused by improper sample machining or surface contaminations. The presented results are the average of contact angles measured on the two sides of the same sample.

A dissolution test equipment was assembled to investigate dissolution reactions between the nitrided steel samples and stationary SAC305 solder melt. The schematic image of the equipment is shown in Fig. 1.

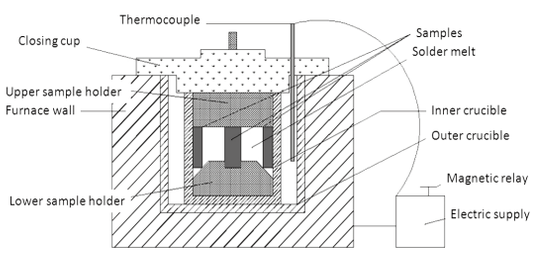

Figure 1*. Schematic image of the assembled dissolution test equipment [22,23]*

The reaction zone of the equipment is inside the inner crucible in which 6 samples were stabilized by the lower and upper sample fixers. The samples and the fixers were submerged into the molten SAC305 solder alloy. To protect the furnace, the inner crucible was placed in an outer crucible. The role of the outer crucible is to act as a protective barrier in the case the inner crucible cracked. The sample fixers, inner and the outer crucibles were made of borosilicate glass that resists thermal shock. Another advantage of borosilicate glass is that the solder melt frozen on the crucible could be easily removed after the tests. The furnace surrounding the outer crucible was a resistance heated tube furnace. The temperature was set with a PID controller and thermocouples. The temperature of the melt was measured with another thermocouple placed between the inner and the outer crucibles. For thermal insulation, the space between the inner and outer crucible was filled with insulating cotton. To protect the melt from contaminations and to improve thermal insulation, the crucibles were covered with a steel cap. The equipment was powered through a magnetic relay which prevented the furnace from automatic restarting after an undesired blackout. This protection is important because the interruption is noticeable in case of a blackout during testing at night or weekends. This feature ensured that false test durations were avoided. The equipment was suitable to carry out dissolution tests for weeks, operating safely night and day.

Prior to dissolution tests, the solder alloy was melted in an air furnace. The samples and the sample fixers were placed inside the inner crucible while the equipment was still shut down. The solder melt was poured into the cold crucible holding the samples to overspread the samples. The furnace was switched on subsequently. By doing so, the samples were protected from oxidation since they were surrounded with solder by the time they were heated up. No stirring was applied during the dissolution tests. Continuous (operating day and night) dissolution tests were carried out on blank and gas-nitrided DC04, C45, CK60 and S103 samples for 5 and 20 days at 593 K (320°C).

After dissolution tests, the solder melt frozen on the samples' surface was not removed to keep the solder/sample interface intact. Since the thickness of the solder melt frozen on the samples was not uniform, they could not be supported with a soft Cu plate during mechanical sample preparations (which is a commonly applied method to preserve the substrate/nitrided region interface). The samples were mounted in resin and cross sections of the samples were prepared. Standard metallographic preparation was used including sand paper polishing, cloth polishing and etching with 2% Nital.

Microstructure examinations were carried out using a Zeiss Evo MA10 type scanning electron microscope (SEM) equipped with EDAX energy dispersive spectrometry (EDS).

3. Results

3.1 Blank steel samples

First, dissolution tests were performed on blank samples to examine the behavior of the untreated steels. Fig. 2 shows SEM-EDS line scan results with two magnifications taken from the DC04, C45, CK60 and S103 steel/SAC305 interfaces after 5 days of dissolution tests. Fig. 2 a and e represent the results of DC04 steel, b, f those of C45, c, g of CK60 type and d, h of S103 type steels. Fig. 3. shows the results after 20 days of immersion tests in the same arrangement.
It can be seen in Fig. 2 that a zone (referred here to as IMZ), within the mixture of SAC305 and grains of the $FeSn_2$ phase are present formed at the steel/SAC305 solder interface for all four steel types after 5 days of test. The formation of the $FeSn_2$ phase univocally proves that Fe dissolution occurred from the steels into the solder melt during the 5 days of dissolution test. After 20 days of test, the thickness of the IMZ

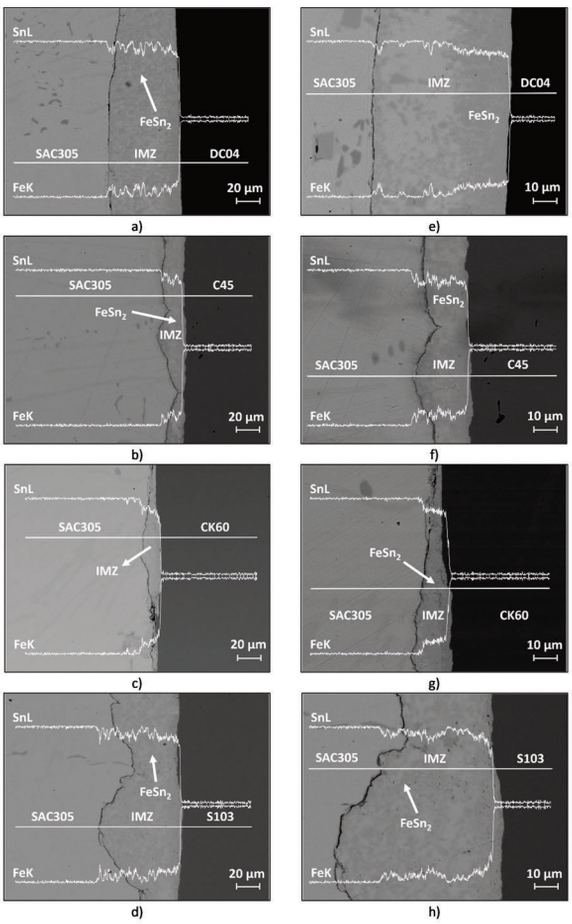

Figure 2. *SEM-EDS line scans across the sample/SAC305 interface of blank a) and e) DC04, b) and f) C45, c) and g) CK60, d) and h) S103 type steels after 5 days of test*

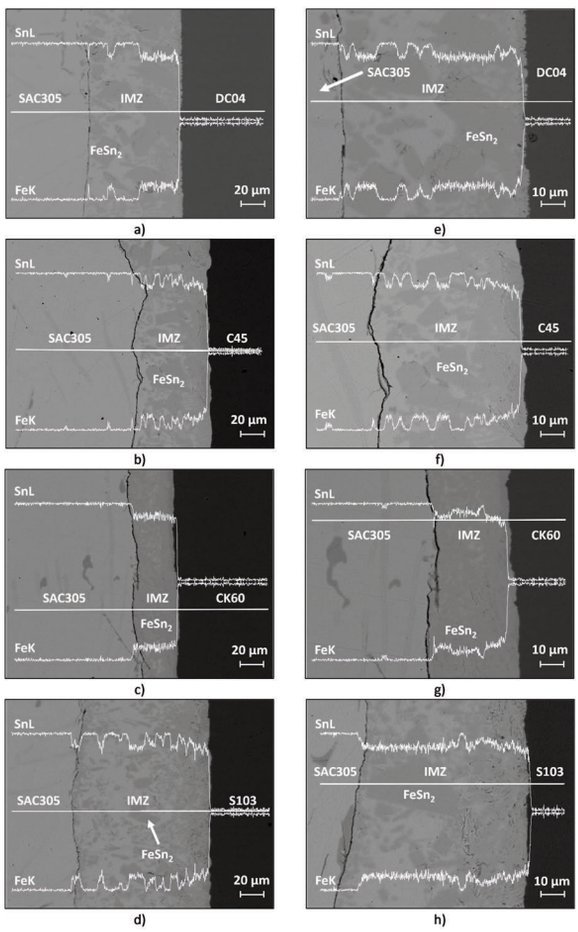

Figure 3. *SEM-EDS line scans across the sample/SAC305 interface of blank a) and e) DC04, b) and f) C45, c) and g) CK60, d) and h) S103 type steels after 20 days of test*

zone is increased (Fig. 3) and within the zone, the grains of $FeSn_2$ are also increased for all steel types. The growth of $FsSn_2$ grains evidenced that Fe dissolution progresses with increasing test duration.

3.1 Gas-nitrided steel samples

The X-ray diffraction spectra obtained from the surfaces of the gas-nitrided steel samples prior to dissolution tests are shown in Fig. 4.

For all four examined steel types, both ε (hexagonal) and γ' (body centered cubic, Fe_4N) iron-nitrides [24] were identified. The reflections of α Fe (ferrite) originate from the substrates. Besides these phases, no other phases were found.

Fig. 5 summarizes the measured contact angles between the SAC305 solder and the gas-nitrided steel samples.

According to Fig. 5, the contact angles are well below 90° for all four steel types, meaning that the wetting between the iron-nitrides formed on the samples and the SAC305 solder melt is good. The contact angles of the gas-nitrided C45, CK60 and S103 steels are close to each other, being between 15°-21°. The best wetting was observed in case of DC04 type steel, where the contact angle was measured to be between 7°-11°.

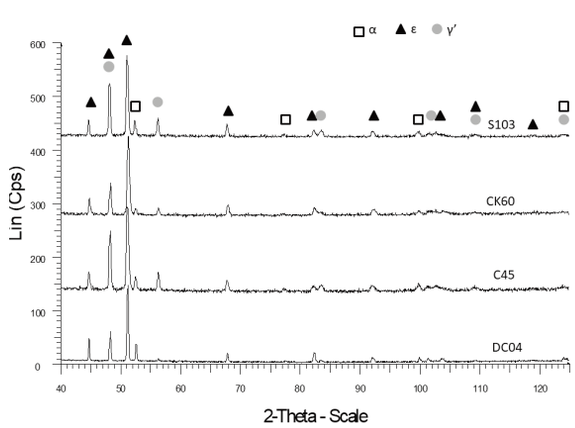

Figure 4. *XRD spectra of the gas-nitrided DC04, C45, CK60 and S103 samples*

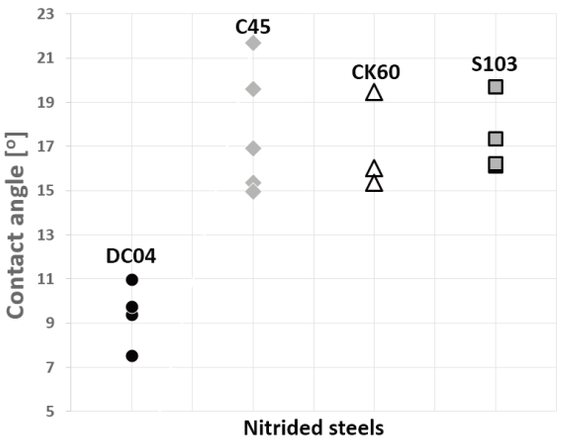

***Figure 5**. Measured contact angles between the gas-nitrided steel samples and SAC305 solder*

The behavior of the gas-nitrided samples submerged into the SAC305 solder alloy melt was investigated through dissolution tests carried out for 5

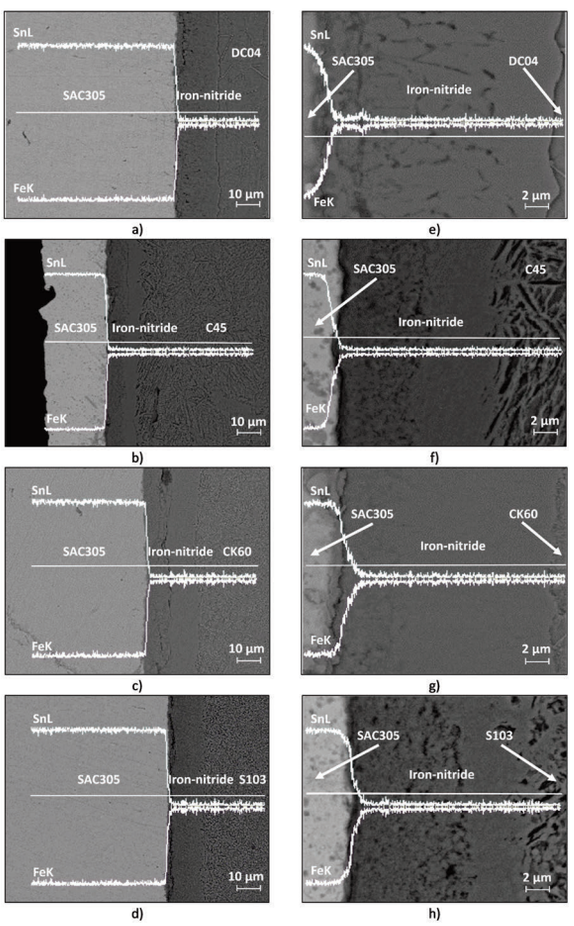

***Figure 6**. SEM-EDS line scans across the sample/SAC305 interface of nitrided a) and e) DC04, b) and f) C45, c) and g) CK60, d) and h) S103 type steels after 5 days of test*

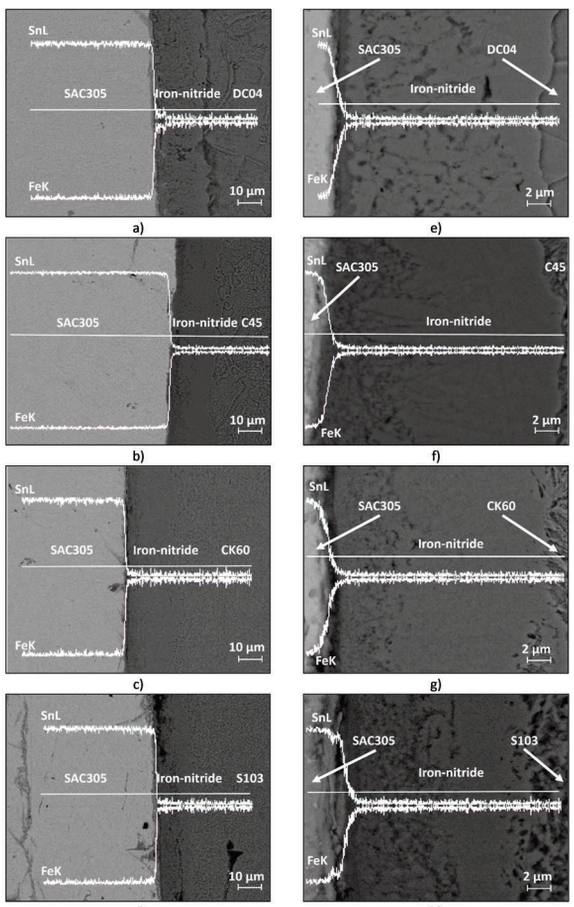

***Figure 7**. SEM-EDS line scans across the sample/SAC305 interface of nitrided a) and e) DC04, b) and f) C45, c) and g) CK60, d) and h) S103 type steels after 20 days of test*

and 20 days. Fig. 6 shows SEM-EDS line scans taken from the gas-nitrided DC04, C45, CK60 and S103 steel/SAC305 interfaces after 5 days of dissolution test. Fig.6 a and e show the results of the DC04 samples, Fig. 6 b and f of C45, Fig. 6 c and g the of CK60 and Fig. 6 d and h the results of S103 samples.

As seen in Fig. 6 a, b, c and d, the $FeSn_2$ intermetallic layer did not form at the solder/sample interface. Furthermore, no other reaction phases or degradation marks are visible. The Fe content is constantly zero within the SAC305 solder at even 50 µm from the solder/sample interfaces, or, in the case of thinner solder drop, (Fig. 6 b) across the whole thickness of the solder drop. Since the Fe content was found to be zero within the SAC305 solder alloy, it can be concluded that Fe dissolution did not take place from gas-nitrided steels into the solder melt.

In Fig. 6, thin cracks parallel with the samples' surface are visible within the iron-nitride layers. These cracks formed during the peeling of the iron-nitride layer. However, no Sn was found inside the formed discontinuities. Thus, peeling did not occur

during the dissolution tests, otherwise, the molten solder would have penetrated into the cracks. The rigid iron-nitride layer is known to tend to peel off during cross section sample preparations if the layer is not sufficiently supported. Since the solder drop frozen on the samples' surface was not flat, the iron-nitride layers could not be supported during sample preparation with the well proven method using flat, soft Cu plates.

Fig. 7 shows the obtained SEM-EDS line scans across the gas-nitrided DC04, C45, CK60 and S103 steels/SAC305 interfaces after 20 days of immersion test. Fig. 7 a and e show the results of the DC04 samples, Fig. 7 b and f of C45, Fig. 7 c and g of CK60 and Fig. 7 d and h results of S103 type samples.

The results obtained after 20 days of dissolution test are very similar to those after 5 days of test. No reaction phases or degradation clues were found after 20 days of test. In the case of all four steel types, the Fe content was found to be zero within the SAC305 solder alloy at even 50 μm from the solder/sample interface. Again, since the Fe content was found to be zero within the SAC305 solder alloy, it can be stated that Fe dissolution did not occur from the samples into the SAC305 solder melt even after 20 days of dissolution tests. Besides that, no sign of any other degradation processes were found.

4. Discussion

Through dissolution tests of blank DC04, C45, CK60 and S103 type steel samples in stationary SAC305 solder melt it was proved that the dissolution of Fe atoms into the SAC305 solder melt occurs even after 5 days leading to a visible formation of the $FeSn_2$ intermetallic phase. Gas-nitriding was applied on DC04, C45, CK60 and S103 type steels and the formation of ε and γ' was observed. The dissolution tests of gas-nitrided steel samples in stationary SAC305 solder melt revealed that no Fe dissolution occurred from the gas-nitrided steels into the solder melt after 5 days or even after 20 days of tests. Furthermore, no dissolution of Sn into steel, or any other degradation mechanism was observed. This result is in contrast with the findings of Matsubara et al. and Hattori et al. [25,26], since they found that an Sn-diffused layer formed in the plasma-nitrided layer of austenitic steel after 5 hours of immersion test in SAC305 at 450°C. Furthermore, they observed the detachment of the nitrided layer and consequently, $FeSn_2$ and Ni_3Sn reaction phases were formed. In their papers, plasma nitriding was applied (instead of gas nitriding) on austenitic steels, having notable Cr-content. However, the main difference is that during their nitriding process, only γ' (Fe_4N) and no ε iron-nitride was formed. In addition, CrN, Cr_2N phases were also obtained. The formation of Cr-nitrides probably played a role in inhibiting the formation of the N-rich ε nitride. The remarkable dissolution resistance of gas-nitrided steels observed here can be attributed to the N-rich ε iron-nitride.

To examine the behavior of different iron-nitrides in Sn-based melts, a simplified thermodynamic model was established. For simplicity, the SAC305 solder melt was modelled with liquid Sn. According to the equilibrium phase diagram, the stoichiometry of ε iron-nitride varies within a rather large composition range (Fig. 8.) Thus, the behavior of γ' (Fe_4N) and Fe_2N nitrides was examined.

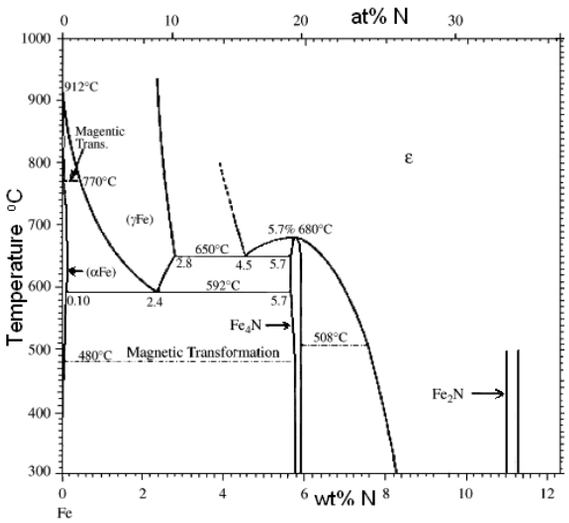

Figure 8. *Section of the Fe-N equilibrium phase diagram [27]*

In Fig.9, three possibilities of steel / liquid Sn contact are schematically shown. In the simplest case, blank steel is in contact with liquid Sn; this is a reactive system at 593 K with the formation of $FeSn_2$ layer (see Table 4 and top Fig.9). During nitriding of steel only Fe_4N is formed on the surface of steel and it comes into contact with liquid Sn; it is much less reactive compared to blank steel, but a slow reaction is still possible (Table 4, middle Fig.9). However, during nitriding the double Fe_4N + Fe_2N layer is formed, the Fe_2N layer is much more stable in liquid Sn (see Table 4 and bottom Fig.9).

Table 4. *Standard Gibbs energy changes of reactions between different states of steel and liquid Sn at T = 593 K calculated from refs. [28-29]*

Reaction	$\Delta_r G^o_{mp}$ kJ/mol-$FeSn_2$	+ 3* kJ/mol
Fe + 2 Sn = $FeSn_2$	-35.4	same -35.4**
0.25 Fe_4N + 2 Sn = $FeSn_2$ + 0.125 N_2	-6.8	-3.8
0.5 Fe_2N + 2 Sn = $FeSn_2$ + 0.25 N_2	-1	2

* this is the energy needed to nucleate a nitrogen bubble. ** in this process no nitrogen bubble is formed

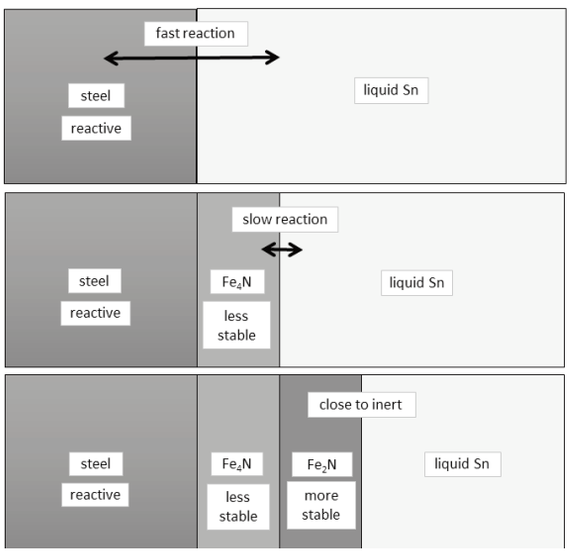

Figure 9. *Three possibilities of steel/liquid Sn contact: blank steel (top figure), nitrided steel with a single Fe_4N layer (middle diagram) and nitrided steel with double Fe_4N + Fe_2N layers (bottom diagram)*

When evaluating the results of Table 4, one should take into account that the chemical reactions between nitrides and liquid Sn will take place only if nitrogen bubbles are formed, for which those bubble should be first nucleated. It is estimated that for a nucleation of a bubble in liquid Sn about +3 kJ/mol extra Gibbs energy is needed. Taking this into account, the results shown in the last column of Table 4 are calculated. It follows that the Fe_2N/Sn interface is stable (the reaction is accompanied with a positive Gibbs energy change), while the Fe_4N/Sn interface is not stable (the reaction is accompanied with a negative Gibbs energy change). Thus, if the outer Fe_2N layer covers the inner Fe_4N layer, then the nitrided steel will be stable in liquid Sn at 593 K. However, if the outer Fe_2N layer is missing, then the nitrided steel will not be stable in liquid Sn but will slowly react.

The presented examinations were carried out with one of the soldering industry's most frequently used Pb-free solder alloys. The reactive nature of Pb-free solder melts in general is attributed to their high Sn content. Since most solder alloys, especially the recently developed environmentally friendly Pb-free solders, are high Sn-containing alloys, ε iron-nitride is expected to show similar dissolution resistance with other Pb-free alloys.

It is generally accepted that good wetting is contributed to those phase systems, where the bond types of the solid and liquid phases are similar. This, for example, stands for most metallic solid /metallic liquid systems, but this is not the case for most ceramic solid/metallic liquid systems. However, it was seen that iron-nitride produced on four steel types with varying C-content showed good wetting with SAC305 solder alloy melt. This suggests that the bond types within iron-nitride are similar in nature to metallic bonds like those of SAC305 solder alloy. However, the detailed characterization of the nature of bond types of iron-nitride is not an aim of the present manuscript.

Finally, it can be concluded that the combination of high resistance against dissolution in Sn-based solder melts and good wetting behavior with high Sn-content solder melts makes gas-nitrided steels/iron potential candidates for hand soldering iron tips and wettable selective wave soldering tool materials. Since gas-nitriding is a widely available treatment nowadays and it is an economic surface treatment method, it can be a reasonable and cost-effective solution to enhance the currently used selective soldering tools' lifetime.

5. Summary

Gas-nitrided DC04, C45, CK60 and S103 type steels showed good wetting with SAC305 solder alloy. The contact angles were between 15°-21° for gas-nitrided C45, CK60 and S103 steels. The lowest contact angles were measured on the DC04 steel, being between 7°-11°.

After 5 and 20 days of dissolution test performed on blank C45 steel submerged into SAC305 solder melt, a notable Fe dissolution was observed by the formation of $FeSn_2$ phase.

No dissolution reaction was observed for gas-nitrided DC04, C45, CK60 and S103 samples after 5 and 20 days of dissolution tests. It can be concluded that gas-nitrided steels/iron show good wetting and excellent dissolution resistance with SAC305 solder melt. The remarkable dissolution resistance was attributed to the formation of ε iron-nitride. These results make nitrided steels/iron potential candidates for hand soldering iron tips and selective soldering tools with enhanced lifetime.

Acknowledgement

The authors would like to thank Zsolt Veres for his aid in the nitriding processes, Peter Baumli for the wetting examinations and Arpad Kovacs for the SEM examinations. Supported by the ÚNKP-17-4 New National Excellence Program of the Ministry of Human Capacities. Some part of the research was supported by the GINOP-2.3.2-15-2016-00027 project. The realization of this project is supported by the European Union and co-financed by the European Social Fund.

References

[1] H. Nishikawa, T. Takemoto, K. Kifune, T. Uetani, N.

Sekimori: Mat Trans, 2004, 45 No 3, pp. 741-746.
[2] Soldering Tips & Lifetime Issues "Coping with Lead Free" (Cooper Industries, Ltd., 2007) http://www.elexp.com/Images/Weller_Coping_with_Lead_Free.pdf. Accessed 4 May 2016
[3] T. Takemoto, T. Uetani, M. Yamazaki: Solder Surf MT Tech, 2004, 16 Iss. 3, pp. 9-15.
[4] H. Nishikawa, S. Kang, T. Takemoto: T JWRI, 2009, 38, No.2, pp. 53-56.
[5] D. Shangguan: Lead-free Solder Interconnect Reliability, 1st ed., ASM International, Ohio, 2005, pp. 6-10.
[6] G. Henshall, J. Bath, C. A. Handwerker: Lead-free Solder Process Development, Wiley & Sons, Hoboken, New Jersey, 2011, pp. 95-99
[7] H. Ipser: JMM 43 B (2), 2007, pp. 109-112.
[8] J. Pstrus: JMM 53 B (3), 2017, pp. 309-318.
[9] A. Kroupa, A.T. Dinsdale, A. Watson, J. Vrestal, A. Zemanova and P. Broz: JMM 48 (3) B, 2012, pp. 339-346.
[10] Soldering Tip Care Tips (Simply Smarter Circuitry Blog)http://www.circuitspecialists.com/blog/soldering-tip-care-tips. Accessed 15 June 2016
[11] H. Nishikawa, A. Komatsu, T. Takemoto: Mat Trans, 2005, 46, pp. 2394-2399.
[12] S. Terashima, Y. Kariya, T. Hosoi, M. Tanaka: J Elect Mat, 2003, 32, pp. 1527-1533.
[13] K. Nogita, T. Nishimura: Sript Mat, 2008, 59, pp. 191-194.
[14] C. M. Gourlay, K. Nogita, J. Read, A. K. Dahle: J Elect Mat, 2009, 39, pp. 56-69.
[15] K. Nogita: Intermet, 2010, 18, pp. 145-149.
[16] Y. Q. WU, S. D. McDonald, J. Read, H. Huang, K. Nogita: Script Mat, 2013, 68, pp. 595-598.
[17] A. A. El-Daly, A. M. El-Taher: Mat Design, 2013, 51, pp. 789-796.
[18] A.A. El-Daly, A.M. El-Taher, T.R. Dalloul: JALCOM, 2014, 587, pp. 32-39.
[19] T.K. Lee, T.R. Bieler, C.-U. Kim, H. Ma.: Fundamentals of Lead-Free Solder Interconnect Technology, Springer, New York, 2015, pp. 21-50.
[20] J. Watanabe, N. Sekimori, K. Hatsuzawa, T. Uetani, I. Shohji: J Phys, Conf. Series, 2012, 379, 012025, pp. 1-10.
[21] Heat Treatment Guide (Boehler Ltd. in Hungarian) http://www.boehler.hu/hungarian/files/1.1221-1.1223.pdf. Accessed 24 June 2016.
[22] Zs. Salyi, M. Benke: Proceedings of the MultiScience - XXX. microCAD International Multidisciplinary Scientific Conference, Hungary, 21-22 April 2016 ISBN 978-963-358-113-1.
[23] Zs. Salyi, Zs. Veres, M. Benke: Proceedings of the Heat Treatment and Materials Science for Mechanical Engineering National Conference and Exhibition with Foreign Participants, Hungary, 5-7 October 2016 ISBN 978-615-5270-31-4.
[24] S. Bhattacharyya: J Phys. Chem. C, 2015, 119, pp. 1601-1622.
[25] N. Matsubara, I. Shohji, H. Kuwahara: Proceedings of the ASME 2011 Pacific Rim Technical Conference & Exposition on Packaging and Integration of Electronic and Photonic Systems, USA, 6-8 July 2011.
[26] S. Hattori, N. Matsubara, I. Shohji, H. Kuwahara: Proceedings of the ASME 2013 International Technical Conference and Exhibition on Packaging and Integration of Electronic and Photonic Microsystems, USA, 16-18 July 2013.
[27] ASM Handbook, Volume 3: Alloy Phase Diagrams, ASM International, 1992.
[28] X. Wang, B. Zhou, Z. Guo, Y. Liu, J. Wang, X. Su: Calphad 57, 2017, pp. 86-97.
[29] A. T. Dinsdale: Calphad 15, 1991, pp. 317-425.
[30] H. Du: J Phase Equil 14, 1993, pp. 682-693.

ISPITIVANJE OTPORA NA RAZLAGANJE KOD UGLJENIČNOG ČELIKA NITRIRANOG GASOM U STACIONARNOM RASTOPU SAC305 LEMA

M. Benke*, Zs. Salyi, G. Kaptay

* Univerzitet u Miškolcu, Institut za fizičku metalurgiju, oblikovanje metala i nanotehnologiju, Miškolc-Egjetemvaroš, Mađarska

Apstrakt

Cilj ove studije je da istraži koliko su određeni čelici nitrirani gasom s promenljivim sadržajem ugljenika odgovarajući kao materijal za alate za selektivno lemljenje s produženim vekom trajanja. ε i γ' nitridi gvožđa formiraju se kada se kaljene i temperovane DC04, C45, CK60 i S103 vrste čelika nitriraju gasom. Merenja kontaktnog ugla pokazala su da sve četiri vrste nitriranog čelika imaju dobru kvašljivost sa SAC305 lemom. Da bi se ispitala reakcija razlaganja između nitriranih vrsta čelika i legure za lemljenje, korišćena je oprema u kojoj su uzorci bili potopljeni u stacionarni SAC305 lem na različite vremenske periode. Uz pomoć skenirajućeg elektronskog mikroskopa i energetsko disperzivne rentgenske spektroskopije traženi su dokazi za reakcije razlaganja, kao i za druge procese degradacije. Uočeno je da se razlaganje Fe nije dogodilo između uzorka i stacionarnog SAC305 lema tokom kontinuiranih testova koji su trajali do 20 dana. Osim toga, tokom eksperimenta nije se dogodila ni jedna vidljiva reakcija razgradnje između uzoraka i lema. Zaključeno je da čelici nitrirani gasom pokazuju dobru kvašljivost u lemovima čija je osnova Sn, što je kombinovano sa izuzetnom otpornošću na razlaganje Fe u lemu koji sadrži visok nivo Sn. Prema tome, čelici/gvožđe nitrirano gasom mogu biti potencijalni materijali za alate za selektivno lemljenje s produženim vekom trajanja.

Ključne reči: *Gvožđe nitrid; Selektivno lemljenje; Kvašenje SAC305; Razlaganje*